Pergamon

Tetrahedron 55 (1999) 12009–12022

TETRAHEDRON

Thionucleoside Disulfides as Covalent Constraints of DNA Conformation

Robert S. Coleman,* Jason L. McCary, and Ronelito J. Perez

Department of Chemistry, The Ohio State University, 100 West 18th Ave., Columbus, Ohio 43210-1185, USA

Received 3 July 1999; accepted 11 August 1999

Abstract: Full details of a new strategy for cross-linking of duplex oligonucleotides are described. A direct base-to-base disulfide bond is formed by oxidation of two appropriately positioned thionucleoside bases. Cross-link formation between 4-thio-2′-deoxyuridine and 6-thio-2′-deoxyinosine is demonstrated in three sequence contexts (3′ to 3′, 5′ to 5′, and opposed). Disulfide formation occurs in high yield in both duplex and hairpin DNA. Molecular modeling and circular dichroism were used to demonstrate minimal distortion of the constrained B-DNA double helix.

Keywords: nucleic acids, thiocarbonyl compounds, disulfides, oligomers, nucleic acid analogs

INTRODUCTION

Elucidation of the relationship of biological function to oligonucleotide structure is an important goal in nucleic acids chemistry.[1] Methods to constrain oligonucleotide conformation have been important as adjuvants in many studies of oligonucleotide structure and function.[2,3,4,5] For example, control of oligonucleotide structure can affect conformational immobilization, reduction of dynamic motion, and stabilization of disfavored conformations.

Such studies can be relevant to elucidating the interaction of DNA with regulatory proteins. For example, within DNA-protein complexes the flexibility of DNA is thought to be increased, and many DNA regulatory proteins induce bends in the DNA duplex when they bind.[6] Some sequences of DNA are inherently bent.[7,8,9,10] Another example of non-canonical DNA folding[11] is the hairpin structures that have been implicated in triplet repeat expansion diseases.[12,13]

The disulfide bond is potentially ideal for covalent cross-linking of DNA because of the ease and reversibility of S–S bond formation and cleavage. The thiol/disulfide redox pair can be manipulated with complete chemoselectivity within biomolecules. Work on disulfides as covalent constraints of oligonucleotide structure comes most prominently from the groups of Glick[14,15,16] and Verdine,[17,18] among several others.[19,20,21] These methodologies use extraneous tethers for supplying the conformational lock (*e.g.*, N^3-(2-thioethyl)thymidine or N^6-(3-thiopropyl)deoxyadenosine) and they have proven extremely useful in studying biomolecular function.[22] Other strategies based on "covalently linked cross-sections" of nucleoside bases have been described by Leonard and co-workers,[23] and very recently by Kishi and co-workers.[24]

*email: coleman@chemistry.ohio-state.edu

0040-4020/99/$ - see front matter
PII: S0040-4020(99)00704-8

In the present work, we describe the full details of a fundamentally distinct and highly effective strategy for cross-linking duplex DNA that is based on a direct, base-to-base disulfide bond between two appropriately positioned thionucleoside bases.[25] This provides the desired covalent cross-link with the absolute minimum number of atoms, which could be advantageous when trying to mimic naturally occurring structures since there is no tether that might interfere sterically. In addition, the short disulfide cross-link prohibits base-flipping out of the double helix, which may prove useful in the examination of DNA processing enzymes such as methyl transferases. Because of the unconventional manner in which the interstrand disulfide is formed, the potential utility of our strategy is complementary to existing protocols that use thiols tethered to the deoxyribose or heterocyclic bases.

In our work, we demonstrate quantitative and reversible formation of disulfide cross-links within duplex DNA using the thionucleoside bases 4-thio-2′-deoxyuridine[26] ($d^{S4}U$) and 6-thio-2′-deoxyinosine[27] ($d^{S6}I$). We examined disulfide formation in three equally effective permutations: (1) $d^{S4}U$–$d^{S4}U$; (2) $d^{S6}I$–$d^{S6}I$; (3) $d^{S4}U$–$d^{S6}I$ (Equation 1), and in three positional contexts with respect to sequence: (1) 3′-oriented; (2) 5′-oriented, and; (3) directly opposed.

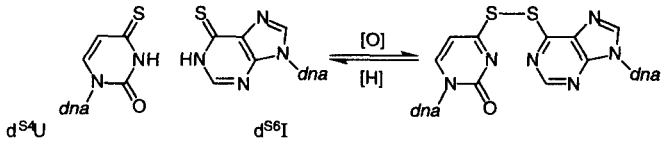

(1)

The incorporation of thionucleosides into synthetic oligodeoxynucleotides is easily achieved by protecting the thiocarbonyl group as the *S*-(2-cyanoethyl) thioimidate,[28] and we have demonstrated the facility with which thionucleosides undergo postsynthetic modification by S-alkylation and disulfide formation.[25,29]

Results

Molecular Modeling. In the molecular modeling and design phase for introduction of 4-thio-2′-deoxyuridine disulfides into duplex DNA, we needed to develop stretching, bending, and torsional constants of the interstrand disulfide bond since the thioimidate substructure was not parameterized effectively in the AMBER* force field.[30,31] The conformation about the disulfide bond critically effects the orientation of the thionucleoside bases relative to the DNA helix. Using the AMBER* molecular mechanics force-field that had been parameterized to accurately handle the thioimidate disulfide,[32] we examined the topology of the thiocarbonyl groups in the starting duplexs and evaluated the distortion of the B-DNA double helix induced upon disulfide bond formation. The energetic contributors to helix distortion are the N^3–C^4–S–S and C^4–S–S–C^4 torsions of d^{S4} U (and the N^1–C^6–S–S and C^6–S–S–C^6 angles in d^{S6}I), which have energy minima at 0° and between 80-100°, respectively. The barriers for rotation about these bonds are 7.2 and 7.9 kcal/mol, respectively.

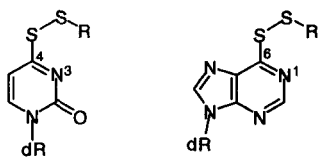

5′d(C A T G G C C A T G)3′
3′d(G T A C C G G T A C)5′

5′d(C A T G X C C A T G)3′
3′d(G T A C Y G G T A C)5′

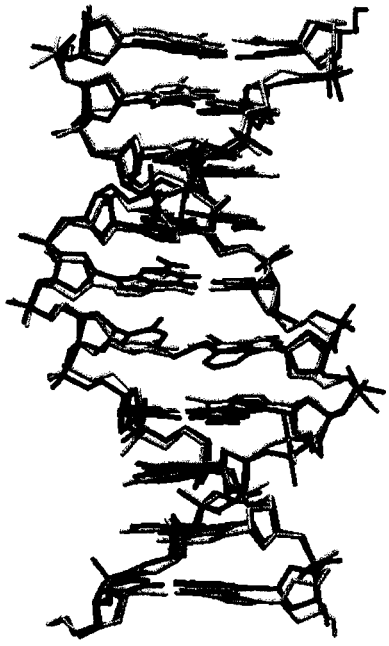

Figure 1. Overlay of molecular dynamics simulations of the $d^{S4}U{\cdot}d^{S6}I$ cross-linked DNA (dark) with natural DNA (light).

Interstrand Thionucleoside Disulfides. Experimentally, rapid and high-yielding formation of disulfide cross-links could be achieved by oxidation of the annealed duplex with an I_2/satd KI solution. Reactions were essentially instantaneous at 25 °C in the presence of excess oxidant, or at least were complete within the time required to work-up a reaction and load it onto a polyacrylamide gel or HPLC column (*e.g.*, within 10 min). Other oxidants such as O_2 or various diazenes were much less effective for disulfide formation with respect to yield or rate. Cross-linking was analyzed by 20% denaturing polyacrylamide gel electrophoresis (PAGE) and quantitated digitally using a phosphorimager.

opposed

5′d(T A A T A C G A C N C A C T A T A)3′
3′d(A T T A T G C T G N G T G A T A T)5′

Within duplex DNA where the mean plane of the bases within a base pair is parallel, a compromise between these two dihedral angles and the stacking of neighboring bases must be reached if the thionucleoside disulfide does not unwind the DNA. Typically, with $d^{S4}U$ disulfide cross-links, molecular modeling using modified AMBER* parameters showed the C^4–S–S–C^4 torsion to fall in the range 55-75°, or reasonably close to its equilibrium value, and the N^3–C^4–S–S torsion to be in the range 20-90°, or distorted to a significant degree from its preferred value of 0°.[33] Distortion of the thionucleosides and adjacent bases relative to the helix involved propeller and buckle motions.[34]

There are two methods that we used to evaluate and correlate molecular modeling studies with experimental data. First, examination of average sulfur-to-sulfur distances in the energy minimized starting *bis*-thionucleoside systems provided an indirect measure of the duplex distortion induced upon cross-link formation. We assumed that the energetic penalty for distortion is proportional to the movement required for the two sulfur atoms to come within bonding distance. In a large macromolecule, this is likely the case for small distortions, although the energetic cost of this distortion would not be linear with respect to distance. Second, the distortion induced upon cross-link formation could be directly evaluated using molecular dynamics simulations, although the energetic cost of distortion would be difficult to quantitate, but examination of the helical parameters compared to non-cross-linked DNA would serve as a qualitative measure.

Using the easily evaluated parameter of sulfur-to-sulfur distance, we found that 5′-disposed *bis*-$d^{S4}U$ residues would be more readily positioned to form interstrand disulfide bonds (S to S distance: 3.5-4.5 Å) compared to the less favorably 3′-disposed bases (S to S distance: 5.5-6.5 Å). This is expected for two groups positioned in the major groove of B-DNA. The S to S distance for the opposed *bis*-$d^{S4}U$ system was 3.5-4.5 Å. Disulfide formation between two $d^{S4}U$ bases induced less helix distortion with a pyrimidine positioned opposite to the $d^{S4}U$ bases, because this arrangement created the conformational flexibility necessary to attain bonding distance.

In support of our contention that a disulfide cross-link would not cause the DNA duplex to deviate significantly from B-form conformation, molecular dynamics simulations showed that a $d^{S4}U$·$d^{S6}I$ disulfide cross-link did not induce any noticeable change in the overall duplex structure. The cross-link was incorporated into the 12-mer B-DNA sequence shown below, whose X-ray structure had been solved by Dickerson and coworkers.[35] Inclusion of the $d^{S4}U$·$d^{S6}I$ cross-link (X = $d^{S4}U$; Y = $d^{S6}I$) was done after initial restricted (0.1 kcal, all atom) minimization of the X-ray structure to relieve strain present from the crystallization forces. This was followed by 1.5 nsec of molecular dynamics at 300 K using the GB/SA water treatment with explicit Na^+ counter-ions positioned equidistant from the phosphate anionic oxygen atoms. Dynamics were carried out until the overall energy stabilized for at least 300 psec. Analysis of the disulfide cross-link showed a slight twisting of the two thionucleoside residues as a consequence of torsions about the N3–C4–S–S, and C–S–S–C bonds. The resulting structure was then compared to the minimized X-ray data obtained from the Brookhaven Protein Data Bank by overlaying all phosphorous atoms along the two DNA backbones. The resulting RMS deviation was 0.6 Å, which we feel demonstrates that there is minimal distortion of the overall duplex structure as a result of incorporation of the disulfide cross-link.

5′-disposed

5′ d(T A A T A C G A C N C A C T A T A) 3′
3′ d(A T T A T G C T G C N T G A T A T) 5′

3′-disposed

5′ d(T A A T A C G A C N C A C T A T A) 3′
3′ d(A T T A T G C T N C G T G A T A T) 5′

For systems with opposed and 5′-disposed *bis*-d^{S4}U bases (N = d^{S4}U), cross-linking was effectively quantitative, with measured yields ≥ 90% (Figure 2, Lanes 2 and 3). The 3′-disposed system underwent cross-linking in poor yield (30%) as a consequence of the energetically disfavored geometry that is required for disulfide formation to occur, even though a pyrimidine base was in the position complementary to the thionucleosides. This was correlated with the longer S to S distance in minimized models of the *bis*-d^{S4}U 3′-disposed system (5.5-6.5 Å) versus the much shorter distance in the 5′-disposed and directly opposed systems (3.5-4.5 Å).

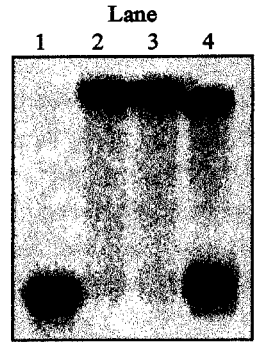

Figure 2. Denaturing PAGE of 4-thio-2′-deoxyuridine disulfide cross-linked duplexes. Lane 1: ^{32}P end-labeled –C^{S4}UC– control; Lane 2: 5′-disposed cross-link; Lane 3: opposed cross-link; Lane 4: 3′-disposed cross-link.

When a purine residue (*e.g.*, dG or dA) was positioned complementary to d^{S4}U bases in a 5′-disposed sequence [*e.g.*, 5′-d(C^{S4}UA)-3′·3′-d(GA^{S4}U)-5′], cross-linking yields were reduced significantly to 60-70%. This result was in line with our modeling observations that showed a normal Pu·Py base pair was not sufficiently mobile to allow the two thiocarbonyl groups to approach close enough to form a covalent bond.

The positional dependence of cross-link formation partly disappeared for *bis*-d^{S6}I systems (N = d^{S6}I), reflective of the decreased duplex distortion that occurs upon disulfide formation. Cross-linking yields ranged from 82-83% for the opposed and 3′-disposed thionucleosides to quantitative (≥ 95%) for the 5′-disposed system (Figure 3). These results are in accord with molecular modeling predictions, which demonstrated S–S bond formation could occur without major distortion of the B-DNA double helix and with close to equilibrium

torsional angles about the thionucleoside disulfide. In the *bis*-$d^{S6}I$ system, the 3′, 5′, and opposed orientations all showed relatively short S to S distances (3.0-5.0 Å) in energy minimized models.

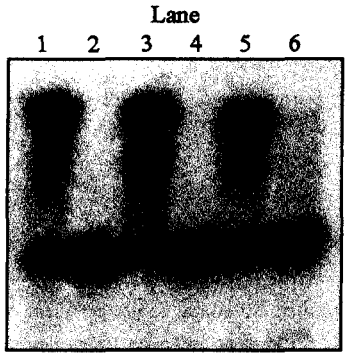

Figure 3. Denaturing PAGE of 6-thio-2′-deoxyinosine disulfide cross-linked duplexes. Lane 1: 3′-disposed cross-link; Lanes 2, 4, and 6: ^{32}P end-labeled –$C^{S6}IC$– control; Lane 3: 5′-disposed cross-link; Lane 5: opposed cross-link.

The mixed $d^{S6}I$–$d^{S4}U$ sequences (X = ^{S6}I; Y = ^{S4}U) were essentially sequence independent with respect to the yield of cross-link formation, again reflective of modeling predictions (Figure 4). In the case of the 3′-disposed system, cross-linking occurred in 85% yield, whereas with the opposed and 5′-disposed cases cross-linking was quantitative (≥ 95% respectively). Modeling had predicted that the opposed $d^{S6}I$–$d^{S4}U$ cross-link would have the best combination of low duplex distortion and optimal disulfide dihedral angles, but even the less optimal systems were demonstrated to be capable of forming disulfide cross-links in excellent yields.

opposed

5′ d(A A T A C G A **X** A C A C T A T A T) 3′
3′ d(T T A T G C T **Y** T G T G A T A T A) 5′

5′-disposed

5′ d(A A T A C G A **X** A C A C T A T A T) 3′
3′ d(T T A T G C T **C** **Y** G T G A T A T A) 5′

3′-disposed

5′ d(A A T A C G A **X** A C A C T A T A T) 3′
3′ d(T T A T G C **Y** C T G T G A T A T A) 5′

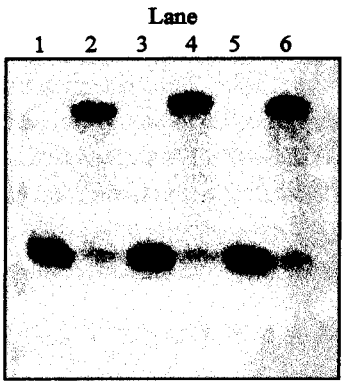

Figure 4. Denaturing PAGE of mixed 4-thiouridine/6-thioinosine disulfide cross-linked duplexes. Lanes 1, 3, and 5: ^{32}P end-labeled –A^{S6}IA– control; Lane 2: opposed cross-link; Lane 4: 5′-disposed cross-link; Lane 6: 3′-disposed cross-link.

DNA hairpin conformations could be covalently constrained with a *bis*-thionucleoside disulfide (Figure 5). Two d^{S4}U bases incorporated in the opposed orientation into the stem region of a hairpin-forming oligonucleotide[36] (N = d^{S4}U; bases in loop italicized) underwent cross-link formation in quantitative yield. The DNA was 5′-end labeled with ^{32}P (Lane 1) and treated with I_2/KI, which effected quantitative formation of the more highly mobile disulfide-locked hairpin (Lane 2). Evidence that cross-linking occurred within a hairpin rather than a duplex was obtained by thermal denaturation of the native DNA at 95 °C, followed by rapid cooling to room temperature (2 min) prior to oxidation (Lane 3). The disulfide cross-link could be rapidly reduced by treatment with dithiothreitol (DTT) (Lane 4).

5′ d (A G N C T A *T G G G T* T A G N C T) 3′

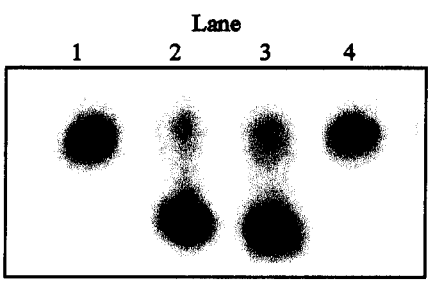

Figure 5. Denaturing PAGE separation of native and disulfide cross-linked hairpin (N = d^{S4}U). Lane 1: native DNA; Lane 2: treatment with I_2/KI, 25 °C; Lane 3: rapid cooling heat denatured DNA followed by treatment with I_2/KI; Lane 4: DTT treatment of disulfide cross-linked DNA from Lane 2.

In another illustration of the versatility of this methodology, we examined the competition between hairpin and duplex cross-linking in a completely self-complementary oligodeoxynucleotide (N = d^{S4}U, bases in loop

italicized). In these experiments, we could preferentially cross-link either the duplex or hairpin structures by controlling the formation for oligonucleotide secondary structure (Figure 6). By rapidly cooling thermally denatured oligomer under no-salt conditions at low DNA concentrations (4.0×10^{-6} μM) followed by iodine oxidation, the cross-linked hairpin conformation could be preferentially obtained in high yield (Lane 2; 80%). Under high salt conditions (0.1 M NaCl) and higher DNA concentrations (3.0×10^{-4} μM) with a slow thermal annealing (95 to 25 °C over 1.5-2 h) and subsequent oxidation with I_2/KI, we could form cross-linked duplex with reasonable selectivity and in good yield (Lane 3; 80%). Since disulfide cross-link formation is reversible, this results in a structural motif transposition of two available secondary structures.

5′ d(A N C A G T *A T A T* A C T N C T) 3′

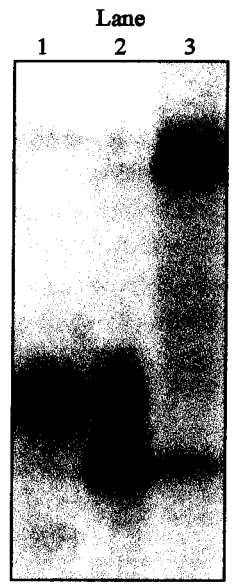

Figure 6. Denaturing PAGE separation of native, cross-linked duplex and cross-linked hairpin conformations of oligonucleotide (N = $d^{S4}U$). Lane 1: native DNA; Lane 2: cross-linked hairpin DNA; Lane 3: cross-linked duplex DNA.

Although molecular modeling proved valuable in the design and evaluation of the cross-linking studies, the near positional independence of disulfide formation led us to conclude that S to S distance was an overly simplified criteria to use. It seemed that the driving force of disulfide formation overrode a significant degree of unfavorable helix distortion. Just how much distortion could be tolerated before disulfide bond formation became unfavorable, if in fact there was a limit, was the most difficult issue to evaluate in efforts to use molecular modeling in our studies. Helical distortion would likely be manifested in kinetic issues whereas the yield of disulfide bond formation is a thermodynamic one. Modeling provided at best a maximum distance beyond which disulfide formation was significantly less effective.

Characterization of Disulfide-Linked Duplexes. Melting studies in 0.1 M NaCl showed the expected large increase in melting temperature (T_m) upon interstrand disulfide formation (Figures 7 and 8). For example, ΔT_m = 37 °C for the 5′-disposed $d^{S4}U{\cdot}d^{S4}U$ system, Figure 5. We found no correlation between the expectedly unrelated parameters of cross-linking yield and T_m of non-cross-linked duplex. All melting curves were reversible and monitoring the absorbance at 320 nm (for duplexes) or 308 nm (for disulfide cross-links) gave identical T_m values.

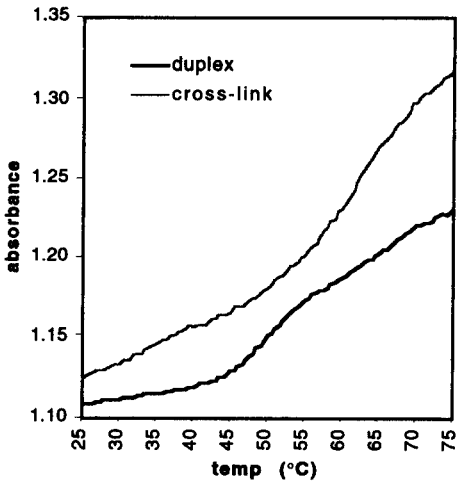

Figure 7. Helix coil transition plot for $d^{S4}U$-$d^{S6}I$ system with bases directly opposed. Duplex: T_m = 44 °C; cross-link: T_m = 65 °C.

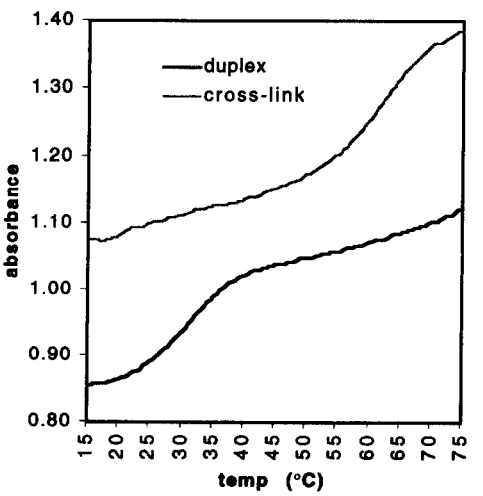

Figure 8. Helix coil transition plot for *bis*-$d^{S4}U$ system with bases 5′-disposed. Duplex: T_m = 31 °C cross-link: T_m = 68 °C.

Analysis of the cross-linked duplex by enzymatic digestion was not possible because the disulfide bond of the parent *bis*-$d^{S4}U$-disulfide was highly sensitive to reducing agents present in commercial enzyme preparations.[37] However, digestion of the disulfide cross-linked duplex according to standard conditions[38] afforded the expected ratio of dG/dA/dC/T/$d^{S4}U$, which clearly showed the presence of the thionucleoside, and on occasion, trace amounts of 2′-deoxyuridine.

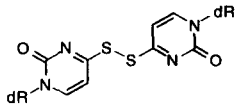

dR = 2-deoxyribofuranoside

Stability of the disulfide bond within duplex DNA in pH 8 buffer at 25 °C, measured by denaturing PAGE, ranged from ≈20% degradation at 48 h for the *bis*-$d^{S4}U$ systems to 0% degradation at 48 h for the *bis*-$d^{S6}I$ systems. When cross-linked samples of DNA were kept dry (lyophylized), the cross-link was indefinitely stable. Examination of the $d^{S4}U$-dimer prepared synthetically by iodine oxidation of $d^{S4}U$ showed this system to be much less stable by itself, compared to its stability in a DNA duplex. ^1H NMR studies of the $d^{S4}U$-dimer showed that after a period of 30 h in aqueous solution, the dimer was transformed into a 1:1 mixture of 2′-deoxyuridine and 4-thio-2′-deoxyuridine, which suggested that oxidation occurred in aqueous (D_2O) solution to afford a sulfur species that is readily hydrolyzed. Suspecting oxygen as the most likely culprit, we found that degassing the D_2O by a repetitive freeze-pump-thaw cycling increased the half-life of the disulfide dimer in solution to approximately 400% of its original value.

Circular dichroism studies showed that the disulfide cross-link did not significantly distort the B-DNA helix. Besides the disappearance of the weak absorption at 320-330 nm attributable to loss of the thiocarbonyl group, there were no significant differences between the CD spectra of the oxidized and reduced systems. The positive ellipticity at 282 nm characteristic of B-DNA underwent a slight red-shift (1-3 nm) upon disulfide formation in all cases, although the interpretation of this shift is not unambiguous (39). In any case, other workers have drawn identical conclusions using circular dichroism that were corroborated by other experimental techniques. Clearly, however, in our case, circular dichroism studies showed no major distortion of the B-DNA double helix upon disulfide formation, consistent with molecular mechanics calculations and molecular dynamics simulations.

CONCLUSION

This methodology for cross-linking oligonucleotides has potential applicability to problems in oligonucleotide structure, for example as a constraint in sequence dependent DNA bending studies. Because of the high reduction potential of the thioimidate disulfide and low oxidation potential of the corresponding thioamide, this methodology may prove useful as a rapidly activated trigger or latch for kinetic studies on RNA folding. Incorporation of thionucleosides into DNA is straightforward, and the protocol for disulfide bond formation is rapid, quantitative, and reversible. Our protocol complements existing work on constrained

DNA duplexes because the cross-link is introduced without the use of extraneous tethers. In optimal positional contexts, the thionucleoside disulfide induces only a minimal distortion of the B-DNA double helix.

EXPERIMENTAL SECTION

HPLC. Oligonucleotides were purified by reverse-phase HPLC on a Hamilton PRP-1 column (4.6 mm × 25 cm, mobile phases: A = 0.1 M triethylammonium acetate, pH 6.5; B = CH_3CN) using a Perkin Elmer Model 250 Biocompatible LC pump, an LC-290 spectrophotometric detector and an PE Nelson 1022 Plus computing integrator.

Synthesis of Oligodeoxyribonucleotides. Oligodeoxynucleotides were synthesized using an Applied Biosystems 392 DNA/RNA synthesizer with commercial reagents and protocols on a 0.2 or 1.0 μmol scale. Standard phosphoramidite chemistry with β-cyanoethyl protecting groups and standard solid-phase synthesis protocols were used. For the incorporation of 6-thio-2′-deoxyinosine and 4-thio-2′-deoxyuridine, the corresponding *S*-cyanoethyl phosphoramidites[13,14] were coupled at the desired position. *O*- and *S*-cyanoethyl phosphate protecting groups were deprotected with 1 M 1,8-diazabicyclo[5.4.0]undec-7-ene (DBU) in CH_3CN (25 °C, 3 h) while the oligonucleotide was attached to the solid support. Cleavage from the support and base deprotection was accomplished with conc. NH_4OH containing 50 mM NaSH (25 °C, 4 h). Following HPLC purification of the 5′-tritylated oligomer (95-50% A over 40 min), the product fraction was lyophilized and detritylated with 80% acetic acid (350 μL, 25 °C, 1 h). The solution was concentrated to dryness, taken up in 0.4 mL of H_2O, and passed through a 0.2 μm membrane filter (Gelman 0.2 μm Acrodisc LC13), and the final oligonucleotide product was re-isolated by HPLC (92-75% over 30 min).

^{32}P End-Labeling of DNA. [γ-^{32}P]ATP was purchased from Amersham. A solution of oligonucleotide (0.1 OD_{260} in H_2O (15 μL) was treated with kinase buffer (10 x, for a final concentration of 5 mM DTT, 10 mM $MgCl_2$, 75 mM Tris, pH 7.5), T4 polynucleotide kinase (0.5 μL, 5 U) and [γ-^{32}P]ATP (1 μL, 7000 Ci/mol, 6.4 μCi/μL) and the reaction mixture was incubated at 37 °C. After 1 h, the reaction mixture was warmed to 65 °C for 5 min then recooled to 25 °C. The solution was diluted to 200 μL with water and passed through a 0.8 mL column of Sephadex G-25 DNA grade resin.

Disulfide Cross-Link Formation The –CNC– and –AXA– containing oligomers were ^{32}P end-labeled and purified using a Sephadex G25 spun column prior to use. Formation of interstrand disulfide cross-links was achieved by addition of approximately $4.0e^{-6}$ μmol of labeled strand to 1-100 equiv of non-labeled complimentary DNA. Duplex DNA solutions were made 0-5 mM in NaCl/H_2O (total DNA concentration = 10 μM) prior to heating at 65 °C for 5 minutes and slow cooling (1 h) to 25 °C. Oxidation was initiated by adding 1 mM I_2/satd. KI solution to bring the total I_2 concentration to 200 μM. Reactions were complete within 10 min

at 25 °C. For reduction of the disulfide, the oxidized sample was treated with 2-4 μL of a 1 mM solution of dithiothreitol followed by dilution (50%) with denaturing loading buffer.

Electrophoresis Polyacrylamide gel electrophoresis was carried out under the following conditions: 0.5 mm gel thickness, 20% acrylamide, 7 M urea, 20% formamide in TBE buffer (50 mM Tris borate, pH 8.3, 1 mM EDTA). Gels were run at constant power (18 W) using TBE as the running buffer. Gel loading dye was 98% formamide containing 0.025% each of xylene cyanol and bromophenol blue. For PAGE experiments, electrophoresis grade acrylamide was pretreated with 0.5 mM aqueous I_2 prior to polymerization to remove unidentified reducing agents. This significantly improved the resolution of the gels by reducing streaking of bands. Gels were scanned using a Molecular Dynamics phosphorimager and the bands were quantitated using ImageQuant™ software. The brightness and contrast of the resulting image was increased to improve legibility using Adobe Photoshop v. 3.0, and the figures were printed as TIFF files on a high-resolution laser printer. The ratio of image intensity to signal over the entire range was linear, and was not significantly effected by electronic processing.

T_m Measurements DNA helix-coil transitions were measured on a Beckman DU-660 spectrophotometer equipped with a Peltier melting apparatus, using 10 mm path-length cuvettes and the Beckman software program. Equal amounts of each strand were mixed in buffer (3-5 μM). Cross-linked samples were purified by Sephadex and/or HPLC before T_m measurements. All melting samples had a final volume of 200 μL and were buffered to pH 7.0 using 0.1 M $KHPO_4$ containing 0.1 M NaCl. These samples were warmed at 95 °C for 5 min and allowed to cool slowly back to room temperature prior to melting experiments. Samples were loaded into cuvettes and allowed to equilibrate at 15 °C for 5 min prior to melting. Melting was performed from 15-75 °C, with a gradient of 0.5 °C/min. Measurements were recorded every 0.5-1.0 min. All experiments were done in triplicate, and experimental T_m values varied ≤1 °C between runs.

CD Spectroscopy. Spectra were obtained on a JASCO J500C spectropolarimeter using 600 μL of a 10 μM solution of duplex DNA in 0.1 M NaCl in pH 7.0 phosphate buffer at 25 °C. The same concentrations of DNA were used for native and cross-linked DNA.

Molecular Modeling. For computer modeling studies, a Silicon Graphics Indigo2 Impact R10000 computer and the commercial program MacroModel (v 5.5) was used. The AMBER* force field, modified as described,[30] was used. Sodium counter-ions were positioned at the appropriate bifurcated geometry relative to the phosphate diesters and all structures were minimized to convergence (RMS ≤ 0.01 kJ/Å·mol).

***bis*-4-Thio-2′-deoxyuridine.** A solution of 4-thio-2′-deoxyuridine (10 mg, 0.041 mmol) in 3 mL of pH 8.0 phosphate buffer at 0 °C was treated with 3.25 mL (0.032 mmol, 0.8 equiv) of 0.1 M I_2 in satd. aqueous KI solution. The reaction mixture was stirred for 15 min at 0 °C, washed with toluene (4 x 25 mL) and concen-

trated *in vacuo*. The white powder was purified by flash chromatography (3 x 2 cm silica, 0-40% $MeOH/CH_2Cl_2$) to afford the disulfide (18.2 mg, 91%) as a white solid: ^1H NMR (250 MHz, D_2O) δ 8.26 (d, J = 7.0 Hz, 1H, C6-H), 6.92 (d, J = 7.0 Hz, 1H, C5-H), 6.08 (m, 1H, C1′-H), 4.30 (m, 1H, C3′-H), 4.05 (m, 1H, C4′-H), 3.76 (m, 2H, C5′-H), 2.52 (m, 2H, C2′-H).

ACKNOWLEDGMENT. This work was supported by a grant from the NIH (GM-47991). R.S.C. was an Alfred P. Sloan Foundation Research Fellow (1995-98).

REFERENCES AND NOTES

1. Sinden, R. R. "DNA Structure and Function," Academic Press (London); 1994.
2. Maglott, E. J.; Glick, G. D. *Nucleic Acids Res.* **1998**, *26*, 1301.
3. Altmann, S.; Labhardt, A. M.; Bur, D.; Lehmann, C.; Bannwarth, W.; Billeter, M.; Wüthrich, K.; Leupin, W. *Nucleic Acids Res.* **1995**, *23*, 4827.
4. Herrlein, M. K.; Nelson, J. S.; Letsinger, R. L. *J. Am. Chem. Soc.* **1995**, *117*, 1015.
5. Wolff, S. A.; Verdine, G. L. *J. Am. Chem. Soc.* **1993**, *115*, 12585.
6. Werner, M. H.; Gronenborn, A. M.; Clore, G. M. *Science* **1996**, *271*, 778.
7. Crothers, D. M. *Science* **1994**, *266*, 1819.
8. Dickerson, R. E.; Goodsell, D. S.; Neidle, S. *Proc. Natl. Acad. Sci. USA* **1994**, *91*, 3579.
9. Erie, D. A.; Yang, G.; Schultz, H. C.; Bustamante, C. *Science* **1994**, *266*, 1562.
10. Grzeskowiak, K. *Chem. Biol.* **1996**, *3*, 785.
11. van Holde, K.; Zlatonova, J. *BioEssays* **1993**, *16*, 59.
12. Mariappan, S. V. S.; Garcia, A. E.; Gupta, G. *Nucleic Acids Res.* **1996**, ***24***, 775.
13. Chen, X.; Mariappan, S. V. S.; Catasi, P.; Ratliff, R.; Moyzis, R. K.; Laayoun, A.; Smith, S. S.; Bradbury, E. M.; Gupta, G. *Proc. Natl. Acad. Sci. USA* **1995**, *92*, 5199.
14. Cain, R. J.; Glick, G. D. *Nucleic Acids Res.* **1997**, *25*, 836.
15. Osborne, S. E.; Völker, J.; Stevens, S. Y.; Breslauer, K. J.; Glick, G. D. *J. Am. Chem. Soc.* **1996**, *48*, 11993.
16. Wang, H.; Osborne, S. E.; Zuiderweg, E. R. P.; Glick, G. D. *J. Am. Chem. Soc.* **1994**, *116*, 5021.
17. Ferentz, A. E.; Keating, T. A.; Verdine, G. L. *J. Am. Chem. Soc.* **1993**, *115*, 9006.
18. Ferentz, A. E.; Verdine, G. L. *J. Am. Chem. Soc.* **1991**, *113*, 4000.
19. Gao, H.; Yang, M.; Cook, A. F. *Nucleic Acids Res.* **1995**, *23*, 285.
20. Azhayeva, E.; Axhayev, A.; Guzaev, A.; Hovinen, J.; Lönnberg, H. *Nucleic Acids Res.* **1995**, *23*, 1170.
21. Milton, J.; Connolly, B. A.; Nikiforov, T. T.; Cosstick, R. *J. Chem. Soc.; Chem. Commun.* **1993**, 779.
22. Verdine, G. L.; Chopra, R.; Harrison, S. C. *Science* **1998**, *282*, 1669.

23. Leonard, N. J.; Bhat, B.; Wilson, S. R.; Cruickshank, K. A. *J. Am. Chem. Soc.* **1991**, *113*, 1398 and references therein.
24. Qiao, X.; Kishi, Y. *Angew. Chem., Int. Ed.* **1999**, *38*, 928-931.
25. Coleman, R. S.; McCary, J. L.; Perez, R. J. *Tetrahedron Lett.* **1999**, *40*, 13.
26. Coleman, R. S.; Siedlecki, J. M. *J. Am. Chem. Soc.* **1992**, *114*, 9229.
27. Coleman, R. S.; McCary, J. L.; Arthur, J. C. *Tetrahedron* **1997**, *53*, 11191.
28. Coleman, R. S.; Siedlecki, J. M. *Tetrahedron Lett.* **1991**, *32*, 3033.
29. Coleman, R. S.; Kesicki, E. A. *J. Am. Chem. Soc.* **1994**, *116*, 11636.
30. Weiner, S. J.; Kollman, P. A.; Case, D. A.; Singh, U. C.; Chio, C.; Alagona, G.; Profeta, S.; Weiner, P. *J. Am. Chem. Soc.* **1984**, *106*, 765.
31. Weiner, S. J.; Kollman, P. A.; Case, D. A. *J. Comput. Chem.* **1986**, *7*, 230.
32. Coleman, R. S.; McCary, J. L. *Bioorg. Med. Chem. Lett.* **1998**, *8*, 3039.
33. Details of molecular modeling studies will be published separately: Coleman, R. S.; McCary, J. L.; unpublished studies.
34. Packer, M. J.; Hunter, C. A. *J. Mol. Biol.* **1998**, *280*, 407, and references therein.
35. Goodsell, D. S.; Kopka, M. L.; Cascio, D.; Dickerson, R. E. *Proc. Nat. Acad. Sci.* **1993**, *90*, 2930.
36. Muller, J. G.; Zheng, P.; Rokita, S. E.; Burrows, C. J. *J. Am. Chem. Soc.* **1996**, *118*, 2320.
37. Coleman, R. S.; McCary, J. L.; unpublished studies.
38. Eadie, J. S.; McBride, L. J.; Efcavitch, J. W.; Hoff, L. B.; Cathcart, R. *Anal. Biochem.* **1987**, *165*, 442.
39. For contrasting interpretations of the origin of small magnitude shifts in CD studies on duplex DNA, see: (a) Malinge, J.-M.; Pérez, C.; Leng, M. *Nucleic Acids Res.* **1994**, *22*, 3834. (b) Erlanson, D. A.; Glover, J. N. M.; Verdine, G. L. *J. Am. Chem. Soc.* **1997**, *119*, 6927.